Energy Efficiency Optimization for a Multiuser IRS-aided MISO System with SWIPT

Jie Tang, *Senior Member*, *IEEE*, Ziyao Peng, Daniel K. C. So, *Senior Member*, *IEEE*, Xiuyin Zhang, *Fellow*, *IEEE*, Kai-Kit Wong, *Fellow*, *IEEE*, and Jonathon Chambers, *Fellow*, *IEEE*

***Abstract*—Combining simultaneous wireless information and power transfer (SWIPT) and an intelligent reflecting surface (IRS) is a feasible scheme to enhance energy efficiency (EE) performance. In this paper, we investigate a multiuser IRS-aided multiple-input single-output (MISO) system with SWIPT. For the purpose of maximizing the EE of the system, we jointly optimize the base station (BS) transmit beamforming vectors, the IRS reflective beamforming vector, and the power splitting (PS) ratios, while considering the maximum transmit power budget, the IRS reflection constraints, and the quality of service (QoS) requirements containing the minimum data rate and the minimum harvested energy of each user. The formulated EE maximization problem is non-convex and extremely complex. To tackle it, we develop an efficient alternating optimization (AO) algorithm by decoupling the original nonconvex problem into three subproblems, which are solved iteratively by using the Dinkelbach method. In particular, we apply the successive convex approximation (SCA) as well as the semi-definite relaxation (SDR) techniques to solve the non-convex transmit beamforming and reflective beamforming optimization subproblems. Simulation results verify the effectiveness of the AO algorithm as well as the benefit of deploying IRS for enhancing the EE performance compared with the benchmark schemes.**

***Index Terms*—Energy efficiency (EE), intelligent reflecting surface (IRS), simultaneous wireless information and power transfer (SWIPT), power splitting (PS).**

I. Introduction

DUE to the device proliferation and dramatic traffic explosion in the Internet-of-Things (IoT) era, wireless communication systems need to meet a variety of quality of service (QoS) requirements, including high spectral efficiency (SE) and high demanding data rate [1], [2]. Meanwhile, in order to achieve green and sustainable wireless communication, energy efficiency (EE) has been viewed as a key indicator for designing wireless communication systems. Recently, an intelligent reflecting surface (IRS) has been considered to be another effective technology to support energy-efficient wireless communication for B5G/6G wireless communication networks [3], [4]. In practice, an IRS is composed of numerous low-cost reconfigurable reflecting units. With an IRS controller, those reflecting units can intelligently and independently steer the amplitude and phase of the incident signal to facilitate the transmission of wireless signals, and thus the wireless signal propagation can be collaboratively altered to enhance the desirable signals and suppress the undesirable interfering signals. In short, with reduced hardware cost and energy consumption, an IRS can efficiently improve wireless communication quality.

Based on the above benefits, using an IRS has been extensively investigated in diverse wireless communication systems [5]–[15]. The authors in [5] optimized the transmit beamforming and the reflect beamforming of an IRS-aided multiple-input single-output (MISO) system with the aim to minimize the total transmit power. Furthermore, the authors in [6] and [7] investigated an IRS-aided multiple-input multiple-output (MIMO) system. Specifically, in [6], the fundamental capacity limit was characterized in a point-to-point MIMO communication network. Additionally, the authors in [7] maximized the weighted sum rate (WSR) in a multicell MIMO system by utilizing the block coordinate descent (BCD) algorithm. In addition, an IRS-aided millimeter wave (mmWave) system has also been widely studied. For example, the authors in [8] maximized the network throughput under the deep reinforcement learning (DRL)-based design, and the authors in [9] applied an alternating manifold optimization algorithm to maximize the WSR, respectively. In addition, an IRS has been employed in other application scenarios such as in heterogeneous networks [10], [11], TeraHertz (THz) communication systems [12], [13], and unmanned aerial vehicle (UAV) systems [14], [15].

On the other hand, to achieve energy-efficient wireless communication, simultaneous wireless information and power transfer (SWIPT) is also seen as a significant approach due to its capability of transmitting data and providing power simultaneously. In a SWIPT wireless communication system,

This work has been supported in part by the National Key Research and Development Program of China under Grant 2019YFB1804100, in part by the National Natural Science Foundation of China under Grant 61971194, 62222105, in part by the Special Project for Guangxi Science and Technology Bases and Talents under Grant AD21075054, in part by the Open Research Fund of Guangdong Key Laboratory of Aerospace Communication and Networking Technology under Grant 2018B030322004, in part by the International Science and Technology Cooperation Project of Guangzhou (Huangpu) under Grant 2020GH06, and in part by the Special Project for Guangxi Science and Technology Bases and Talents under Grant AD21075054. This article was presented in part at IEEE Global Communications Conference (GLOBECOM), 04-08 December 2022 [DOI: 10.1109/GLOBECOM48099.2022.10000645]. (*Corresponding author: Ziyao Peng.*)

Jie Tang, Ziyao Peng and Xiuyin Zhang are with the School of Electronic and Information Engineering, South China University of Technology, Guangzhou 510641, China (e-mail: eejtang@scut.edu.cn; 202120112366@mail.scut.edu.cn; zhangxiuyin@scut.edu.cn).

Daniel K. C. So is with the School of Electrical and Electronic Engineering, University of Manchester, Manchester M13 9PL, U.K. (e-mail: d.so@manchester.ac.uk).

Kai-Kit Wong is with the Department of Electronic and Electrical Engineering, University College London, London WC1E 6BT, U.K. (e-mail: k.wong@ee.ucl.ac.uk).

Jonathon Chambers is with the Department of Engineering, University of Leicester, Leicester LE1 7RH, U.K. (e-mail: jonathon.chambers@ncl.ac.uk).

there are generally two feasible approaches for the receiver named time switching (TS) and power splitting (PS) to realize information decoding (ID) and energy harvesting (EH) [16]–[21]. For the TS scheme, the authors in [16] jointly optimized the TS factors and the transmit covariance matrices in a two-user SWIPT MISO system employing the TS scheme to investigate the achievable rate region. Additionally, the authors in [17] studied a TS-based NOMA system with SWIPT and developed a dual-layer algorithm to maximize the EE by reasonably designing the TS factors and power allocation. For the PS scheme, the authors in [18] studied a SWIPT-enabled MIMO system, in which the transmit beamformers, receive filters, as well as the power splitters were designed to minimize the total transmit power. In [19], by optimizing PS ratios and transmit power, a PS-based SWIPT distributed antenna system has been investigated to maximize the EE considering both cases of single or multiple IoT devices. In addition, the authors in [20] and [21] considered both the TS and PS approaches in the SWIPT system. Especially, the authors in [20] investigated the outage performance, and the authors in [21] analyzed the throughput performance and outage probability. In general, the performance comparison between the TS scheme and the PS scheme is not deterministic, which depends on actual application scenarios, the optimization objective, and so on.

With the immense potential of an IRS and SWIPT to improve energy efficiency, there have been several significant works on the combination of these two techniques [22]–[28]. The authors in [22] first studied the IRS-aided SWIPT system for the purpose of maximizing the weighted sum power of the EH receivers. In [23], the total BS transmit power of an IRS-aided MISO system with SWIPT was minimized under perfect and imperfect CSI. Furthermore, the authors in [24] employed the difference of convex functions (DC) programming, majorization-minimization (MM) approach, and manifold optimization to maximize the EE indicator of an IRS-aided MISO system with SWIPT, while considering the maximum transmit power budget and IRS unit-modulus constraints. On the other hand, there have been other significant studies for IRS-aided SWIPT systems focusing on transmit power minimization [25], weighted sum rate maximization [26], and EE maximization problems in the systems with two different user categories, i.e. information users and energy users [27], [28]. To our best knowledge, the EE maximization problem for an IRS-aided PS-based SWIPT system considering the QoS constraints has not been studied yet. On the other hand, PS theoretically achieves better rate-energy tradeoffs than TS [29], thus motivating this paper.

Motivated by the above research, we investigate a PS-based SWIPT system, where the IRS is positioned between the BS and the users to improve the communication environment with the aim to maximize the EE. To efficiently tackle the EE optimization issue, we develop an alternating optimization (AO) algorithm by jointly optimizing the transmit beamforming vectors, the reflective beamforming vector, and the PS ratios separately in an alternating manner. The following are our main contributions:

- We investigate a multiuser MISO IRS-aided system with SWIPT, where we apply the PS scheme to all the users. The BS transmit beamforming, the IRS reflective beamforming, as well as the power distribution for each user are mathematically modeled such that they can be synthetically designed to enhance the EE performance while satisfying the maximum transmit power budget, the IRS reflection constraint, as well as the QoS constraints at the users. However, the EE maximization problem becomes extremely complicated because of the coupling of all the optimization variables, and thus is difficult to solve.
- To efficiently deal with the EE maximization problem, we propose an AO algorithm by decoupling the original problem into three subproblems, i.e., transmit beamforming optimization, reflective beamforming optimization, and PS ratios optimization. For each subproblem, the Dinkelbach method is applied to deal with the non-convex fractional programming issue. Particularly, for the transmit and reflective beamforming optimization subproblems, the successive convex approximation (SCA), as well as the semi-definite relaxation (SDR) techniques are applied to convert the non-convex problems into convex problems, allowing us to solve them using the standard convex optimization solver CVX [30].
- The effectiveness and the superiority of the AO algorithm are demonstrated by simulation results. Furthermore, compared with benchmark schemes with random reflective beamforming or without the IRS, the benefit of deploying IRS for enhancing the EE performance can be demonstrated by our findings.

Organization: We organize the remaining part of this paper as follows. In Section II, we present the multiuser MISO IRS-aided SWIPT system model and formulate the EE maximization problem. In Section III, an efficient AO algorithm is proposed to tackle the non-convex and extremely complex EE optimization problem. Subsequently, we provide the simulation results in Section IV. Finally, we give the conclusions of our work in Section V.

Notations: Boldface upper letters, boldface lower letters, and lower letters represent matrices, vectors, and scalars, respectively. For a square matrix $\mathbf{Q}$, the notations $\mathbf{Q}^T$, $\mathbf{Q}^H$, $\mathrm{rank}(\mathbf{Q})$ and $\mathrm{Tr}(\mathbf{Q})$ represent its transpose, hermitian conjugate transpose, rank, and trace. $\mathbf{Q} \preceq \mathbf{0}$ and $\mathbf{Q} \succeq \mathbf{0}$ indicate $\mathbf{Q}$ is negative or positive semidefinite, respectively. $\mathbf{0}$ and $\mathbf{I}_M$ denote the all-zero matrix and an $M \times M$ identity matrix. $\mathbb{C}^{x\times y}$ denotes an $x \times y$ dimensional complex matrices and $\mathrm{diag}(a_1, ..., a_N)$ indicates a diagonal matrix, respectively. In addition, $|a|$ represents the magnitude of a complex number a and $\|\boldsymbol{b}\|$ represents the Euclidean norm of vector $\boldsymbol{b}$. Let $\mathcal{CN}(\boldsymbol{\mu},\mathbf{C})$ indicate the distribution of a circularly symmetric complex Gaussian (CSCG) random vector with mean $\boldsymbol{\mu}$ and covariance matrix $\mathbf{C}$.

II. System Description and Problem Formulation

A. System Description

As illustrated in Fig.1, we investigate a multiuser IRS-aided MISO system with SWIPT, which contains one BS equipped with M transmit antennas, one IRS composed of N passive

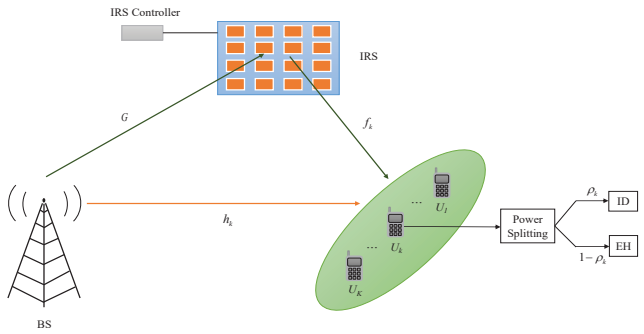

Fig. 1. Illustration of a multiuser IRS-aided MISO system with SWIPT.

reflecting units, and K single-antenna users. Specially, we denote the set of passive reflecting units and the set of all users as $\mathcal{N} \triangleq \{1, \ldots, N\}$ and $\mathcal{K} \triangleq \{1, \ldots, K\}$. Furthermore, we assume that each user is equipped with an EH rectification circuit and a conventional ID circuit.

The quasi-static flat-fading model is taken into account for all the channels. Furthermore, it is assumed that both the BS and IRS controller are capable of obtaining the perfect channel state information (CSI). [1] Let $\boldsymbol{G} \in \mathbb{C}^{N\times M}, \boldsymbol{f}_k \in \mathbb{C}^{N\times 1}$ and $\boldsymbol{h}_k \in \mathbb{C}^{M\times 1}$ represent the channel matrix of the BS-IRS link and the channel vectors of the IRS-user k and BS-user k link, respectively. For user k, let $s_k \sim \mathcal{CN}(0,1)$ and $\boldsymbol{w}_k \in \mathbb{C}^{M\times 1}$ denote the intended message with unit-power and the corresponding transmit beamforming vector, respectively. Accordingly, we can formulate the transmitted signal as

$$\boldsymbol{x} = \sum_{k=1}^{K} \boldsymbol{w}_k s_k. \tag{1}$$

To guarantee that the transmit power does not exceed the maximum value P_T, the optimization problem is limited by

$$\mathrm{E}(\|\boldsymbol{x}\|^2) = \sum_{k=1}^{K} \|\boldsymbol{w}_k\|^2 \le P_T. \tag{2}$$

As for IRS, we denote the reflection-coefficients matrix as $\boldsymbol{\Phi}$ = diag $\left(\gamma_1 e^{j\phi_1}, \ldots, \gamma_N e^{j\phi_N}\right)$, where $\phi_n \in [0, 2\pi)$ and $\gamma_n \in [0, 1]$ are the phase shift and the reflection amplitude of the n-th reflecting unit, respectively. In addition, let $\boldsymbol{v} = \left[\gamma_1 e^{j\phi_1}, \ldots, \gamma_N e^{j\phi_N}\right]^H$ represent the reflective beamforming vector, in which $|v_n| = \left|\gamma_n e^{j\phi_n}\right| \le 1, \forall n \in \mathcal{N}$. Therefore, the combined BS-user k reflective channel can be written as $\boldsymbol{f}_k^H \boldsymbol{\Phi} \boldsymbol{G} = \boldsymbol{v}^H \boldsymbol{\Psi}_k$, where $\boldsymbol{\Psi}_k$ = diag$\left(\boldsymbol{f}_k^H\right)$ $\boldsymbol{G}$.

Based on the PS scheme, the signals received by each user are split into two power streams: one stream is used for EH, and the other stream is used for ID. For user k, let $\rho_k (0 < \rho_k < 1)$ denote the part of the received signal power for ID, and the $1-\rho_k$ part is for EH. Under this setup, by combining reflected signals and the directly transmitted signals, the signal received at user k can be expressed as

$$y_k^{ID} = \sqrt{\rho_k} \sum_{i=1}^{K} (\boldsymbol{v}^H \boldsymbol{\Psi}_k + \boldsymbol{h}_k^H) \boldsymbol{w}_i \boldsymbol{s}_i + n_k, \tag{3}$$

where $n_k \sim \mathcal{CN}(0, \sigma_k^2)$ denotes the additive white Gaussian noise (AWGN).

Furthermore, we treat the interference of the system as noise, thus formulating the achievable data rate for user k as

$$R_k^{ID} = \log_2 \left(1 + \frac{\rho_k \left| \left(\boldsymbol{v}^H \boldsymbol{\Psi}_k + \boldsymbol{h}_k^H \right) \boldsymbol{w}_k \right|^2}{\rho_k \sum\limits_{i=1, i\neq k}^{K} \left| \left(\boldsymbol{v}^H \boldsymbol{\Psi}_k + \boldsymbol{h}_k^H \right) \boldsymbol{w}_i \right|^2 + \sigma_k^2} \right). \tag{4}$$

Hence, we can express the total achievable rate of the proposed system as

$$\begin{aligned} R_{total} &= \sum_{k=1}^{K} R_k^{ID} \\ &= \sum_{k=1}^{K} \log_2 \left(1 + \frac{\rho_k \left| \left(\boldsymbol{v}^H \boldsymbol{\Psi}_k + \boldsymbol{h}_k^H \right) \boldsymbol{w}_k \right|^2}{\rho_k \sum\limits_{i=1, i\neq k}^{K} \left| \left(\boldsymbol{v}^H \boldsymbol{\Psi}_k + \boldsymbol{h}_k^H \right) \boldsymbol{w}_i \right|^2 + \sigma_k^2} \right). \end{aligned} \tag{5}$$

In addition, the energy harvested by user k can be expressed as

$$e_k = \eta (1 - \rho_k) \sum_{i=1}^{K} \left| (\boldsymbol{v}^H \boldsymbol{\Psi}_k + \boldsymbol{h}_k^H) \boldsymbol{w}_i \right|^2, \tag{6}$$

where $0 < \eta \le 1$ denotes the energy conversion efficiency. In general, it is more practical to consider a nonlinear EH model, but the input power is typically small in SWIPT system due to the signal attenuation [33]. For low input power, SWIPT systems work in the linear region of the nonlinear model, and the nonlinear EH model can be approximated by a linear model [34].

Therefore, we can write the total harvested energy as

$$E = \sum_{k=1}^{K} e_k = \sum_{k=1}^{K} \eta (1 - \rho_k) \sum_{i=1}^{K} \left| (\boldsymbol{v}^H \boldsymbol{\Psi}_k + \boldsymbol{h}_k^H) \boldsymbol{w}_i \right|^2. \tag{7}$$

In general, the harvested energy at all the users can compensate for part of the power consumption in a SWIPT system [17]. As a result, the total power consumption is given by

$$P_{total} = \zeta \sum_{k=1}^{K} \|\boldsymbol{w}_k\|^2 + M P_M + N P_n(b) + P_C - E, \tag{8}$$

where $\zeta = \kappa^{-1}$ with κ being the transmit power amplifier drain efficiency [35], P_M is the power consumption of each transmit antenna, $P_n(b)$ is the power consumption per reflecting unit of the IRS having b-bit resolution [35] and P_C is the circuit power consumption.

Define the EE of the communication system as the ratio of the total achievable rate and the total power consumption. Hence, we can formulate the EE of the proposed system with PS scheme as equation (9).

[1] Though the perfect CSI is an ideal assumption, it is still meaningful for us to characterize the EE performance of the IRS-aided SWIPT system. In general, to acquire the CSI, there are a series of channel estimation schemes for IRS-aided MISO systems based on signal processing techniques such as deep learning, compressed sensing, alternating least squares, and so on [31], [32].

$$\lambda_{EE} \triangleq \frac{R_{total}}{P_{total}} = \frac{\sum_{k=1}^{K} R_k^{ID}}{\zeta \sum_{k=1}^{K} \|\boldsymbol{w}_k\|^2 + P_C + MP_M + NP_n(b) - E} = \frac{\sum_{k=1}^{K} \log_2\left(1 + \frac{\rho_k \left|\left(\boldsymbol{v}^H \boldsymbol{\Psi}_k + \boldsymbol{h}_k^H\right)\boldsymbol{w}_k\right|^2}{\rho_k \sum_{i=1, i\neq k}^{K} \left|\left(\boldsymbol{v}^H \boldsymbol{\Psi}_k + \boldsymbol{h}_k^H\right)\boldsymbol{w}_i\right|^2 + \sigma_k^2}\right)}{\zeta \sum_{k=1}^{K} \|\boldsymbol{w}_k\|^2 + P_C + MP_m + NP_n(b) - \sum_{k=1}^{K} \eta(1-\rho_k) \sum_{i=1}^{K} \left|(\boldsymbol{v}^H \boldsymbol{\Psi}_k + \boldsymbol{h}_k^H)\boldsymbol{w}_i\right|^2} \tag{9}$$

B. Problem Formulation

In this paper, our goal is to maximize the EE of the proposed multiuser IRS-aided MISO system with SWIPT by jointly optimizing the BS transmit beamforming vectors$\{\boldsymbol{w}_k\}$, the IRS reflective beamforming vector $\boldsymbol{v}$ and the PS ratios $\{\rho_k\}$. Particularly, the EE maximization problem is limited by considering the maximum transmit power budget, the IRS reflection constraints, and the QoS requirements dictating the minimum data rate and the minimum harvested energy per user. Mathematically, we can formulate the complete optimization problem as

$$\text{(P1)} \quad \max_{\{\boldsymbol{w}_k\}, \boldsymbol{v}, \{\rho_k\}} \lambda_{\text{EE}} \tag{10}$$

$$\text{s.t.} \quad \log_2\left(1 + \frac{\rho_k \left|\left(\boldsymbol{v}^H \boldsymbol{\Psi}_k + \boldsymbol{h}_k^H\right)\boldsymbol{w}_k\right|^2}{\rho_k \sum_{i=1, i\neq k}^{K} \left|\left(\boldsymbol{v}^H \boldsymbol{\Psi}_k + \boldsymbol{h}_k^H\right)\boldsymbol{w}_i\right|^2 + \sigma_k^2}\right) \geq R_{\min}, \forall k \in \mathcal{K}, \tag{11}$$

$$\eta(1-\rho_k) \sum_{i=1}^{K} \left|(\boldsymbol{v}^H \boldsymbol{\Psi}_k + \boldsymbol{h}_k^H)\boldsymbol{w}_i\right|^2 \geq E_{\min}, \forall k \in \mathcal{K}, \tag{12}$$

$$\sum_{k=1}^{K} \|\boldsymbol{w}_k\|^2 \leq P_T, \tag{13}$$

$$0 < \rho_k < 1, \forall k \in \mathcal{K}, \tag{14}$$

$$|v_n| \leq 1, \forall n \in \mathcal{N}. \tag{15}$$

where inequalities (11) and (12) correspond to the QoS requirements per user. Specifically, equation (11) guarantees the minimum data rate constraint, in which $R_{\min}$ is the minimum rate requirement. Equation (12) guarantees the minimum harvested energy constraint, in which $E_{\min}$ is the minimum harvested energy target.

Since the objective function (10) is an extremely complicated fraction, problem (P1) is non-convex. In addition, the problem consists of three intricately coupled sets of variables, i.e., $\{\boldsymbol{w}_k\}$, $\boldsymbol{v}$, and $\{\rho_k\}$, which makes the problem (P1) intractable and cannot be solved directly.

III. The Proposed AO Algorithm

In this section, we develop an AO algorithm to tackle the complex EE maximization problem (P1) by decoupling problem (P1) into three subproblems, which are solved alternatively. Specifically, we first optimize the transmit beamforming vectors $\{\boldsymbol{w}_k\}$ to obtain a better transmit beam pattern design. Subsequently, based on the fixed $\{\boldsymbol{w}_k\}$, we optimize the reflective beamforming vector $\boldsymbol{v}$ to obtain higher channel gain. Finally, the PS ratio $\{\rho_k\}$ is optimized to enhance the EE performance.

A. Transmit Beamforming Optimization

We first optimize the transmit beamforming vectors $\{\boldsymbol{w}_k\}$ with the fixed reflective beamforming vector $\boldsymbol{v}$ and the PS ratios $\{\rho_k\}$. We define $\boldsymbol{a}_k = \boldsymbol{\Psi}_k^H \boldsymbol{v} + \boldsymbol{h}_k$ as the effective channel of the BS-user k link, $\forall k \in \mathcal{K}$ for notational convenience. Furthermore, we set $\boldsymbol{A}_k = \boldsymbol{a}_k \boldsymbol{a}_k^H$ and $\boldsymbol{W}_k = \boldsymbol{w}_k \boldsymbol{w}_k^H$ with $\boldsymbol{W}_k \succeq \boldsymbol{0}$ and $\text{rank}(\boldsymbol{W}_k) \leq 1, \forall k \in \mathcal{K}$. Therefore, R_k^{ID} and e_k can be reformulated as

$$R_k^{ID'} = \log_2\left(\frac{\rho_k \sum_{i=1}^{K} \text{Tr}(\boldsymbol{A}_k \boldsymbol{W}_i) + \sigma_k^2}{\rho_k \sum_{i=1, i\neq k}^{K} \text{Tr}(\boldsymbol{A}_k \boldsymbol{W}_i) + \sigma_k^2}\right), \tag{16}$$

$$e_k' = \eta(1-\rho_k) \sum_{i=1}^{K} \text{Tr}(\boldsymbol{A}_k \boldsymbol{W}_i). \tag{17}$$

Accordingly, we can express the transmit beamforming optimization problem as

$$\text{(P2)} \quad \max_{\{\boldsymbol{W}_k\}} \lambda'_{EE} \triangleq \frac{R'_{total}}{P'_{total}} = \frac{\sum_{k=1}^{K} R_k^{ID'}}{\zeta \sum_{k=1}^{K} \text{Tr}(\boldsymbol{W}_k) + P_C + MP_M + NP_n(b) - \sum_{k=1}^{K} e_k'} \tag{18}$$

$$\text{s.t.} \quad R_k' \geq R_{\min}, \forall k \in \mathcal{K}, \tag{19}$$

$$e_k' \geq E_{\min}, \forall k \in \mathcal{K}, \tag{20}$$

$$\sum_{k=1}^{K} \text{Tr}(\boldsymbol{W}_k) \leq P_T, \tag{21}$$

$$\boldsymbol{W}_k \succeq \boldsymbol{0}, \forall k \in \mathcal{K}, \tag{22}$$

$$\text{rank}(\boldsymbol{W}_k) \leq 1, \forall k \in \mathcal{K}. \tag{23}$$

Since the objective function (18) is a fraction, problem (P2) is neither convex nor linear. Referring to previous works, the Dinkelbach method [36] is widely used to tackle the fractional

optimization problem; thus we apply it to convert function (18) into a subtractive form. By introducing a parameter q, we can formulate the objective function of problem (P2) as

$$H(q) = \max_{\{\boldsymbol{W}_k\}} R_{total}^{'} - qP_{total}^{'} \tag{24}$$

However, function (24) is still non-convex. To turn problem (P2) into convex form, we introduce new variables as follows,

$$e^{p_k} = \rho_k \sum_{i=1}^{K} \mathrm{Tr}(\boldsymbol{A}_k \boldsymbol{W}_i) + \sigma_k^2, \forall k \in \mathcal{K}, \tag{25}$$

$$e^{q_k} = \rho_k \sum_{i=1, i\neq k}^{K} \mathrm{Tr}(\boldsymbol{A}_k \boldsymbol{W}_i) + \sigma_k^2, \forall k \in \mathcal{K}. \tag{26}$$

Then, we have

$$\begin{aligned} &\sum_{k=1}^{K} \log_2 \left(\frac{\rho_k \sum\limits_{i=1}^{K} \mathrm{Tr}(\boldsymbol{A}_k \boldsymbol{W}_i) + \sigma_k^2}{\rho_k \sum\limits_{i=1, i\neq k}^{K} \mathrm{Tr}(\boldsymbol{A}_k \boldsymbol{W}_i) + \sigma_k^2} \right) \\ &= \sum_{k=1}^{K} \log_2(e^{(p_k - q_k)}) = \sum_{k=1}^{K} (p_k - q_k) \log_2(e). \end{aligned} \tag{27}$$

Accordingly, we can further reformulate problem (P2) as

$$(\text{P2.1}) \max_{\{\boldsymbol{W}_k\}, \{p_k\}, \{q_k\}} \sum_{k=1}^{K} (p_k - q_k) \log_2(e) - qP_{total}^{'} \tag{28}$$

$$\text{s.t.} \quad \rho_k \sum_{i=1}^{K} \mathrm{Tr}(\boldsymbol{A}_k \boldsymbol{W}_i) + \sigma_k^2 \geq e^{p_k}, \forall k \in \mathcal{K}, \tag{29}$$

$$\rho_k \sum_{i=1, i\neq k}^{K} \mathrm{Tr}(\boldsymbol{A}_k \boldsymbol{W}_i) + \sigma_k^2 \leq e^{q_k}, \forall k \in \mathcal{K}, \tag{30}$$

$$(p_k - q_k) \log_2(e) \geq R_{\min}, \forall k \in \mathcal{K}, \tag{31}$$

(20), (21), (22), and (23).

However, problem (P2.1) still can not be directly solved because of the non-convex constraint (23) and (30). Here we use the SCA technique to tackle this issue. The first-order Taylor expansion of e^{q_k} at the point $\bar{q}_k$ is $e^{\bar{q}_k} + e^{\bar{q}_k}(q_k - \bar{q}_k)$, where $\bar{q}_k$ is feasible to the problem (P2.1). Therefore, we can rewrite the constraint (30) as

$$\rho_k \sum_{i=1, i\neq k}^{K} \mathrm{Tr}(\boldsymbol{A}_k \boldsymbol{W}_i) + \sigma_k^2 \leq e^{\bar{q}_k} + e^{\bar{q}_k}(q_k - \bar{q}_k), \forall k \in \mathcal{K}. \tag{32}$$

Furthermore, we apply the SDR technique to relax the non-convex rank-one constraint (23), thus reformulating problem (P2.1) as

$$(\text{P2.2}) \max_{\{\boldsymbol{W}_k\}, \{p_k\}, \{q_k\}} \sum_{k=1}^{K} (p_k - q_k) \log_2(e) - qP_{total}^{'} \tag{33}$$

$$\text{s.t.} \quad \rho_k \sum_{i=1}^{K} \mathrm{Tr}(\boldsymbol{A}_k \boldsymbol{W}_i) + \sigma_k^2 \geq e^{p_k}, \forall k \in \mathcal{K}, \tag{34}$$

$$\rho_k \sum_{i=1, i\neq k}^{K} \mathrm{Tr}(\boldsymbol{A}_k \boldsymbol{W}_i) + \sigma_k^2 \leq e^{\bar{q}_k} + e^{\bar{q}_k}(q_k - \bar{q}_k), \forall k \in \mathcal{K}, \tag{35}$$

$$(p_k - q_k) \log_2(e) \geq R_{\min}, \forall k \in \mathcal{K}, \tag{36}$$

(20), (21), and (22).

For a fixed parameter q, it is obvious that problem (P2.2) is a standard semi-definite programming (SDP), which can be efficiently solved by using CVX. Morever, we denote the optimal solution of problem (P2.2) as $\{\boldsymbol{W}_k^*\}$, then the following proposition can be obtained.

Proposition 1: $\{\boldsymbol{W}_k^*\}$ satisfies $\mathrm{rank}(\boldsymbol{W}_k^*) = 1, \forall k \in \mathcal{K}$.

Proof: The detailed proof is presented in Appendix A. ■

Hence, we can apply eigenvalue decomposition to acquire the beamforming vectors $\{\boldsymbol{w}_k^*\}$. Algorithm 1 provides the optimization algorithm for transmit beamforming.

Algorithm 1 the optimization algorithm for transmit beamforming optimization

0: **INITIALIZE:** $q^{(0)} = 0$, $\boldsymbol{q}^{(0)} = \boldsymbol{0}$. Set iteration number m = 0, n = 0 and ε>0 as the accuracy threshold.
0: **REPEAT:**
0: For a given $q^{(n-1)}$
0: **REPEAT:**
0: For a given $\bar{\boldsymbol{q}}^{(m-1)}$, solve problem (P2.2) to obtain $\{\boldsymbol{W}_k\}^{(m)}$ and $\boldsymbol{q}^{(m)}$
0: Set $\bar{\boldsymbol{q}}^{(m)} = \boldsymbol{q}^{(m)}$, $m = m + 1$
0: **UNTIL** the objective value in problem (P2.2) converges;
0: Calculate the objective value (10) and (33), which are denoted by $\lambda_{EE}^{(n)}$ and $f_1^{(n)}$
0: Set $q^{(n)} = \lambda_{EE}^{(n)}$, $n = n + 1$
0: **UNTIL** converge, i.e. $f_1^{(n)} \leq \varepsilon$
0: **OUTPUT:** Obtain q_1^* and the beamforming vectors $\{\boldsymbol{w}_k^*\}$ by eigenvalue decomposition.

B. Reflective Beamforming Optimization

Similar to Section III-A, we use the SCA and SDR techniques as well as the Dinkelbach method to optimize the reflective beamforming vector $\boldsymbol{v}$ with the fixed transmit beamforming vectors $\{\boldsymbol{w}_k\}$ and the PS ratios $\{\rho_k\}$. Therefore, we define $\boldsymbol{c}_{k,i} = \boldsymbol{\Phi}_k \boldsymbol{w}_i$ and $d_{k,i} = \boldsymbol{h}_k^H \boldsymbol{w}_i, \forall k \in \mathcal{K}, i \in \mathcal{K}$. Then, we have

$$\left| \left(\boldsymbol{v}^H \boldsymbol{\Phi}_k + \boldsymbol{h}_k^H \right) \boldsymbol{w}_i \right|^2 = \boldsymbol{v}^H \boldsymbol{C}_{k,i} \boldsymbol{v} + 2\mathrm{Re}\left\{ \boldsymbol{v}^H \boldsymbol{u}_{k,i} \right\} + |d_{k,i}|^2, \tag{37}$$

where $\boldsymbol{C}_{k,i} = \boldsymbol{c}_{k,i} \boldsymbol{c}_{k,i}^H$, $\boldsymbol{u}_{k,i} = \boldsymbol{c}_{k,i} d_{k,i}^H$. Moreover, we define $\left| \left(\boldsymbol{v}^H \boldsymbol{\Phi}_k + \boldsymbol{h}_k^H \right) \boldsymbol{w}_i \right|^2 = \bar{\boldsymbol{v}}^H \boldsymbol{R}_{k,i} \bar{\boldsymbol{v}} + |d_{k,i}|^2$, where $\boldsymbol{R}_{k,i} = \begin{bmatrix} \boldsymbol{C}_{k,i} & \boldsymbol{u}_{k,i} \\ \boldsymbol{u}_{k,i}^H & 0 \end{bmatrix}$ and $\bar{\boldsymbol{v}} = \begin{bmatrix} \boldsymbol{v} \\ 1 \end{bmatrix}$. In addition, we set $\boldsymbol{V} = \bar{\boldsymbol{v}} \bar{\boldsymbol{v}}^H$ with $\boldsymbol{V} \succeq \boldsymbol{0}$ and $\mathrm{rank}(\boldsymbol{V}) \leq 1$. Therefore, R_k and e_k can be reformulated as

$$R_k^{ID''} = \log_2\left(\frac{\rho_k \sum_{i=1}^{K}(\mathrm{Tr}\,(\boldsymbol{R}_{k,i}\boldsymbol{V}) + |d_{k,i}|^2) + \sigma_k^2}{\rho_k \sum_{i=1,i\neq k}^{K}(\mathrm{Tr}\,(\boldsymbol{R}_{k,i}\boldsymbol{V}) + |d_{k,i}|^2) + \sigma_k^2}\right), \tag{38}$$

$$e_k'' = \eta(1-\rho_k)\sum_{i=1}^{K}(\mathrm{Tr}\,(\boldsymbol{R}_{k,i}\boldsymbol{V}) + |d_{k,i}|^2). \tag{39}$$

Next, the Dinkelbach method is applied to reformulate the reflective beamforming optimization problem as

$$\begin{aligned}(\mathrm{P3}) \max_{\boldsymbol{V}} \quad & R_{total}^{''} - qP_{total}^{''} = \\ & \sum_{k=1}^{K} R_k^{ID''} - q(\zeta \sum_{k=1}^{K} \|\boldsymbol{w}_k\|^2 + P_C + MP_M + NP_n(b) - \sum_{k=1}^{K} e_k'') \end{aligned} \tag{40}$$

$$\begin{aligned} \text{s.t.} \quad & R_k^{ID''} \geq R_{\min}, \forall k \in \mathcal{K}, && (41)\\ & e_k'' \geq E_{\min}, \forall k \in \mathcal{K}, && (42)\\ & \boldsymbol{V} \succeq \boldsymbol{0}, && (43)\\ & \mathrm{rank}(\boldsymbol{V}) \leq 1, && (44)\\ & \boldsymbol{V}_{n,n} \leq 1, \forall n \in \mathcal{N}, && (45)\\ & \boldsymbol{V}_{N+1,N+1} = 1. && (46) \end{aligned}$$

Subsequently, we introduce two sets of new variables i.e.$\{s_k\}$ and $\{t_k\}$ as

$$e^{s_k} = \rho_k \sum_{i=1}^{K}(\mathrm{Tr}\,(\boldsymbol{R}_{k,i}\boldsymbol{V}) + |d_{k,i}|^2) + \sigma_k^2, \forall k \in \mathcal{K}, \tag{47}$$

$$e^{t_k} = \rho_k \sum_{i=1,i\neq k}^{K}(\mathrm{Tr}\,(\boldsymbol{R}_{k,i}\boldsymbol{V}) + |d_{k,i}|^2) + \sigma_k^2, \forall k \in \mathcal{K}. \tag{48}$$

The first-order Taylor expansion of e^{t_k} at the point $\bar{t}_k$ is $e^{\bar{t}_k} + e^{\bar{t}_k}(t_k - \bar{t}_k)$. By using the SCA technique and relaxing the non-convex constraint (44), we can further reformulate problem (P3) as

$$(\mathrm{P3.1}) \max_{\boldsymbol{V},\{s_k\},\{t_k\}} \sum_{k=1}^{K}(s_k - t_k)\log_2(e) - qP_{total}^{''}, \tag{49}$$

$$\text{s.t.} \quad \rho_k \sum_{i=1}^{K}(\mathrm{Tr}\,(\boldsymbol{R}_{k,i}\boldsymbol{V}) + |d_{k,i}|^2) + \sigma_k^2 \geq e^{s_k}, \forall k \in \mathcal{K}, \tag{50}$$

$$\rho_k \sum_{i=1,i\neq k}^{K}(\mathrm{Tr}\,(\boldsymbol{R}_{k,i}\boldsymbol{V}) + |d_{k,i}|^2) + \sigma_k^2 \leq e^{\bar{t}_k} + e^{\bar{t}_k}(t_k - \bar{t}_k), \forall k \in \mathcal{K}, \tag{51}$$

$$(s_k - t_k)\log_2(e) \geq R_{\min}, \forall k \in \mathcal{K}, \tag{52}$$

(42), (43), (45), and (46).

For a fixed parameter q, it is obvious that problem (P3.1) is strictly concave in $\boldsymbol{v}, \{s_k\}, \{t_k\}$, $\forall k \in \mathcal{K}$, and thus we can solve it efficiently by using CVX and obtain the optimal solution to problem (P3.1) denoted by $\boldsymbol{V}^*$. Particularly, if $\mathrm{rank}\,(\boldsymbol{V}^*) \leq 1$, then we can use the eigenvalue decomposition to obtain reflective beamforming vector $\boldsymbol{v}^*$. However, if $\mathrm{rank}\,(\boldsymbol{V}^*) > 1$, then the Gaussian randomization procedure [37] needs to be applied to obtain the solution that satisfies constraint (44). Specifically, we assume that the eigenvalue decomposition of $\boldsymbol{V}^*$ is $\boldsymbol{V}^* = \boldsymbol{F}\boldsymbol{\Lambda}\boldsymbol{F}^H$. We denote $\hat{\boldsymbol{v}} = \boldsymbol{F}\boldsymbol{\Lambda}^{\frac{1}{2}}\boldsymbol{z}$, in which $\boldsymbol{z} \sim \mathcal{CN}(0, \boldsymbol{I})$ is the Gaussian random vector. Under this setup, we can obtain a feasible solution $\bar{\boldsymbol{v}}$ to problem (P3), which can be expressed as $\bar{\boldsymbol{v}}_n = e^{j\arg(\hat{\boldsymbol{v}}_n/\hat{\boldsymbol{v}}_{N+1})}$, where $\bar{\boldsymbol{v}}_n$ and $\hat{\boldsymbol{v}}_n$ are the n-th element of $\bar{\boldsymbol{v}}$ and $\hat{\boldsymbol{v}}$. With a large number of the randomizations, we can select the best solution among them to obtain the near-optimal solution to problem (P3). The optimization algorithm for the reflective beamforming vector optimization is summarized in Algorithm 2.

Algorithm 2 the optimization algorithm for the reflective beamforming vector optimization

0: **INITIALIZE:** $q^{(0)} = q_1^*$, $\boldsymbol{t}^{(0)} = \boldsymbol{0}$. Set iteration number m = 0, n = 0 and ε>0 as the accuracy threshold.
0: **REPEAT:**
0: For a given $q^{(n-1)}$
0: **REPEAT:**
0: For a given $\bar{\boldsymbol{t}}^{(m-1)}$, solve (P3.2) to obtain $\{\boldsymbol{V}\}^{(m)}$ and $\boldsymbol{t}^{(m)}$
0: Set $\bar{\boldsymbol{t}}^{(m)} = \boldsymbol{t}^{(m)}$, $m = m + 1$
0: **UNTIL** the objective value in (P3.2) converges;
0: Calculate the objective value (10) and (49), which is denoted by $\lambda_{EE}^{(n)}$ and $f_2^{(n)}$
0: Set $q^{(n)} = \lambda_{EE}^{(n)}$, $n = n + 1$
0: **UNTIL** converge, i.e. $f_2^{(n)} \leq \varepsilon$
0: **OUTPUT:** Obtain q_2^* and the reflective beamforming vector $\boldsymbol{v}^*$ by eigenvalue decomposition if $\mathrm{rank}\,(\boldsymbol{V}^*) \leq 1$, otherwise use the Gaussian randomization procedure to obtain a solution that satisfies constraint (44).

C. PS Ratios Optimization

By applying the Dinkelbach method to (P1) and fixing the transmit beamforming vectors $\{\boldsymbol{w}_k\}$ and the reflective beamforming vector $\boldsymbol{v}$, we can reformulate problem (P1) as

$$\begin{aligned}(\mathrm{P4}) \max_{\{\rho_k\}} R(\boldsymbol{\rho}) = & \sum_{k=1}^{K} R_k^{ID} - \\ & q(\zeta \sum_{k=1}^{K} \|\boldsymbol{w}_k\|^2 + P_C + MP_M + NP_n(b) - \sum_{k=1}^{K} e_k) \end{aligned} \tag{53}$$

$$\begin{aligned} \text{s.t.} \quad & R_k^{ID} \geq R_{\min}, \forall k \in \mathcal{K}, && (54)\\ & e_k \geq E_{\min}, \forall k \in \mathcal{K}, && (55)\\ & 0 < \rho_k < 1, \forall k \in \mathcal{K}. && (56) \end{aligned}$$

Proposition 2: The objective function (53) is strictly concave in $\rho_k, \forall k \in \mathcal{K}$ with a fixed parameter q.

Proof: The detailed proof is presented in Appendix B. ■

Consequently, the objective function can be reformulated as

$$R(\boldsymbol{\rho}) = \sum_{k=1}^{K} R_k, \tag{57}$$

where

Algorithm 3 the optimization algorithm for the PS ratios optimization

0: **INITIALIZE:** $q^{(0)} = q_2^*$. Set iteration number n = 0 and $\varepsilon>0$ as the accuracy threshold.
0: **REPEAT:**
0: For a given $q^{(n-1)}$
0: Solve the problem (P4.1) to obtain $\boldsymbol{\rho}^*$
0: Calculate the objective value (10) and (59), which are denoted by $\lambda_{EE}^{(n)}$ and $f_3^{(n)}$
0: Set $q^{(n)} = \lambda_{EE}^{(n)}$, $n = n + 1$
0: **UNTIL** converge, i.e. $f_3^{(n)} \leq \varepsilon$
0: **OUTPUT:** q_3^* and $\boldsymbol{\rho}^*$;

$$R_k = R_k^{ID} - q\zeta\|\boldsymbol{w}_k\|^2 - \frac{q}{K}(P_C + MP_M + NP_n(b)) + qe_k. \tag{58}$$

From Proposition 2, we can obtain $\frac{d^2R(\boldsymbol{\rho})}{d\rho_i d\rho_j} = 0, \forall i \neq j$, which means the PS ratio of each user is independent of each other. Thus the maximization problem of $R(\boldsymbol{\rho})$ is equivalent to the maximization problems of R_k for each user. Hence, we can divide problem (P4) into *K* non-interfering subproblems. In general, we can formulate the subproblems of (P4) as

$$(\text{P4.1}) \max_{\{\rho_k\}} \quad R_k(\rho_k) \tag{59}$$

$$\text{s.t.} \quad R_k^{ID} \geq R_{\min}, \forall k \in \mathcal{K}, \tag{60}$$

$$e_k \geq E_{\min}, \forall k \in \mathcal{K}, \tag{61}$$

$$0 < \rho_k < 1, \forall k \in \mathcal{K}. \tag{62}$$

Here we individually maximize $R_k(\rho_k)$ and then obtain a solution set from all the subproblems. According to the constraints (60)-(62), ρ_k should be limited as

$$\rho_k^{\min} \leq \rho_k \leq \rho_k^{\max} \tag{63}$$

where $\rho_k^{\min} = \frac{(2^{R_{\min}}-1)\sigma_k^2}{\left|\left(\boldsymbol{v}^H\boldsymbol{\Phi}_k\boldsymbol{h}_k^H\right)\boldsymbol{w}_k\right|^2 - (2^{R_{\min}}-1)\sum\limits_{i=1,i\neq k}^{K}\left|\left(\boldsymbol{v}^H\boldsymbol{\Phi}_k\boldsymbol{h}_k^H\right)\boldsymbol{w}_i\right|^2} > 0$ ensures that the minimum data rate constraint of user k can be satisfied, and $\rho_k^{\max} = 1 - \frac{E_{\min}}{\eta\sum\limits_{i=1}^{K}\left|\left(\boldsymbol{v}^H\boldsymbol{\Phi}_k\boldsymbol{h}_k^H\right)\boldsymbol{w}_i\right|^2} < 1$ ensures the minimum harvested energy constraint of user k can be satisfied. Furthermore, since $\frac{d^2R(\boldsymbol{\rho})}{d\rho_k^2} < 0, \forall k \in \mathcal{K}$, R_k is strictly concave in ρ_k. Hence, we can obtain a unique root to the equation $\frac{dR(\rho_k)}{d\rho_k} = 0$ denoted by $\hat{\rho}$ to maximize R_k.

In general, the optimal PS ratio of user k can be obtained as follows,

$$\rho_k^* = \begin{cases} \rho_k^{\min}, & \hat{\rho}_k < \rho_k^{\min} \\ \hat{\rho}_k, & \rho_k^{\min} \leq \hat{\rho}_k \leq \rho_k^{\max} \\ \rho_k^{\max}, & \hat{\rho}_k > \rho_k^{\max} \end{cases} \tag{64}$$

Consequently, we can obtain the optimal PS ratios $\{\rho_1^*, \rho_2^*, ..., \rho_K^*\}$ of problem (P4). Algorithm 3 provides the optimization algorithm for the PS ratios.

D. Alternating Optimization of the Optimize Variables $\{\boldsymbol{w}_k\}$, $\boldsymbol{v}$, and $\{\rho_k\}$

Based on the aforementioned three algorithms for solving subproblems, the key steps of the complete AO algorithm flow for tackling the original problem (P1) can be summarized in Algorithm 4.

Algorithm 4 The Complete AO Algorithm

0: **INITIALIZE:** $\left(\{\boldsymbol{w}_k\}^{(0)}, \boldsymbol{v}^{(0)}, \{\rho_k\}^{(0)}\right)$. Set iteration number t = 0 and $\varepsilon>0$ as the accuracy threshold.
0: **REPEAT:**
0: For given $\left(\boldsymbol{v}^{(t-1)}, \{\rho_k\}^{(t-1)}\right)$, solve problem (P2) according to Algorithm 1 in Section III-A and obtain the solution denoted by $\{\boldsymbol{w}_k\}^{(t)}$
0: For given $\left(\{\boldsymbol{w}_k\}^{(t)}, \{\rho_k\}^{(t-1)}\right)$, solve problem (P3) according to Algorithm 2 in Section III-B and obtain the solution denoted by $v^{(t)}$
0: For given $\left(\{\boldsymbol{w}_k\}^{(t)}, \boldsymbol{v}^{(t)}\right)$, solve problem (P4) according to Algorithm 3 in Section III-C and obtain the solution denoted by $\{\rho_k\}^{(t)}$
0: Calculate the objective value (10) denoted by $\lambda_{EE}^{(t)}$
0: Set t = t + 1
0: **UNTIL** converge, i.e. $\left|\lambda_{EE}^{(t)} - \lambda_{EE}^{(t-1)}\right|^2 \leq \varepsilon$

It is worth noting that the strict convergence of the overall AO algorithm can not be guaranteed due to the Gaussian randomization procedure. However, it has been mathematically and numerically proved that a good approximation of the optimal solution can be obtained by the SDR technique followed by Gaussian randomization [see [38] and the references therein]. Therefore, the convergence can be improved by increasing the number of Gaussian randomizations.

E. Computational Complexity Analysis

First, we denote the iteration numbers of the SCA technique for solving problems (P2.2) and (P3.1) as I_{s1} and I_{s2}, and the iteration numbers of the Dinkelbach method for solving problems (P2.2), (P3.1) and (P4.1) as I_{d1}, I_{d2} and I_{d3}, respectively. Note that we can solve Problems (P2.2) and (P3.1) using the interior-point algorithm which is implemented in CVX. According to [39], for an SDP problem containing an $x \times x$ positive semi-definite matrix and y SDP constraints, the computational complexity can be formulated as $\mathcal{O}(\sqrt{x}log(\frac{1}{\tau})(yx^3 + x^2y^2 + y^3))$, where τ denotes the solution accuracy. Therefore, we can obtain the approximate computational complexity for solving (P2.2) and P(3.1) as $\mathcal{O}_1 = \mathcal{O}(log(\frac{1}{\tau})(4K + 1)(M^{3.5} + 4KM^{2.5}))$ and $\mathcal{O}_2 = \mathcal{O}(log(\frac{1}{\tau})(3K + 1)(N^{3.5} + 3KN^{2.5}))$. Since we can directly calculate the PS ratios from (64) to solve problem (P4.1), the involved complexity is $\mathcal{O}_3 = \mathcal{O}(K)$. Above all, the computational complexity of the AO algorithm is $\mathcal{O}(I_{s1}I_{d1}\mathcal{O}_1 + I_{s2}I_{d2}\mathcal{O}_2 + I_{d3}\mathcal{O}_3)$.

IV. Simulation Results and Discussion

In this section, we present simulation results to validate the superiority and the effectiveness of our proposed algorithm in a multiuser IRS-aided MISO system with SWIPT illustrated in Fig. 2, with one BS located at (0,0), one IRS located at (5m, 0) and 3 users (K = 3) located at (5m, -1m), (5m, 1m), (6m,

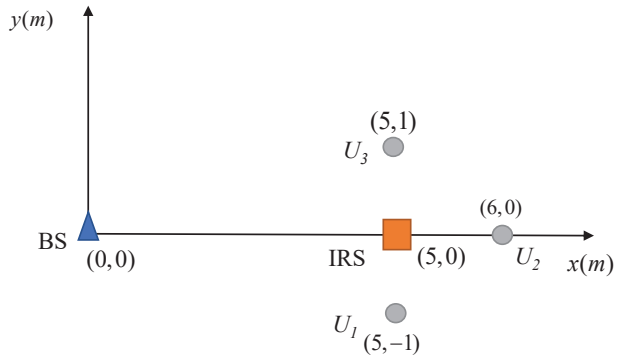

Fig. 2. The simulated multiuser IRS-aided MISO system with SWIPT.

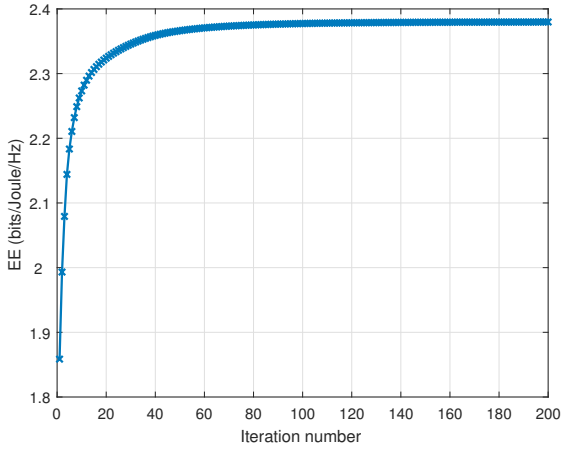

Fig. 3. Convergence performance of the AO algorithm.

TABLE I
SIMULATION PARAMETERS

Parameters	Values
Numbers of users, K	3
Numbers of antenna at the BS, M	3
Numbers of reflecting units, N	16
Received antenna noise, σ_k^2	-40dBm
Maximum transmit power P_T	40dBm
The minimum rate target, R_{min}	1.1 bits/s/Hz
The minimum harvested power requirement constraint, E_{min}	1 μw
The circuit power consumption, P_C	2W
Dissipated power at each transmit antenna, P_M	0.1W
Dissipated power at the n-th IRS element, $P_n(b)$	0.01W
The reciprocal of the transmit power amplifier drain efficiency, ζ	1.2
The energy conversion efficiency, η	0.4

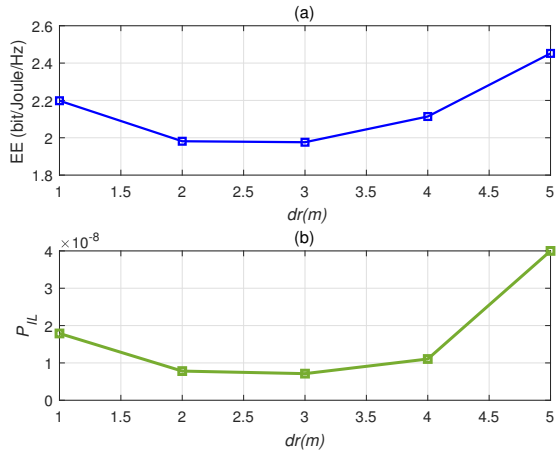

Fig. 4. EE and P_{IL} versus the distance between the BS and the IRS.

0), respectively. Furthermore, the distance-dependent path loss model [40] can be written as

$$P_L = C_0\left(\frac{d}{d_0}\right)^{-\alpha}, \tag{65}$$

where α is the path-loss exponents, which are set to be 3.6, 2, and 2.5 for the BS-user, BS-IRS, and IRS-user links, respectively. Additionally, the reference path loss at $d_0 = 1$m is $C_0 = -30$dB.

Referring to [41], we suppose that the BS-user link follows Rayleigh fading denoted by $\overline{\boldsymbol{h}_k}$, whereas the IRS-aided links follow Rician fading. Furthermore, the IRS and BS are both assumed to be equipped with several half-wavelength uniform linear array (ULA) antenna elements. Accordingly, we can model $\boldsymbol{G}, \boldsymbol{f}_k$, and $\boldsymbol{h}_k$ as

$$\boldsymbol{h}_k = P_{L_{1k}}\overline{\boldsymbol{h}_k}, \tag{66}$$

$$\boldsymbol{G} = P_{L_2}\left(\sqrt{\frac{\tau}{\tau+1}}\boldsymbol{a}_N(\vartheta)\boldsymbol{a}_M(\psi)^H + \sqrt{\frac{1}{\tau+1}}\overline{\boldsymbol{G}}\right), \tag{67}$$

$$\boldsymbol{f}_k = P_{L_{3k}}\left(\sqrt{\frac{\tau}{\tau+1}}\boldsymbol{a}_N(\varsigma_k) + \sqrt{\frac{1}{\tau+1}}\overline{\boldsymbol{f}_k}\right), \tag{68}$$

where $P_{L_{1k}}$, $P_{L_2}$and $P_{L_{3k}}$ represent the corresponding path-losses, ϑ, ψ and ς_k are the angular parameters, $\tau = 10$ and $\boldsymbol{a}$ are the Rician factor and the steering vector, respectively. In addition, $\overline{\boldsymbol{G}}$ and $\overline{\boldsymbol{f}_k}$ are the NLOS components. Table I lists the other simulation parameters and all simulation results are based on the average of over 100 independent channel realizations.

Above all, we investigate the convergence performance of the AO algorithm. As we can see in Fig. 3, with the number of AO iterations increasing, EE can converge to a stable value, thus validating the effectiveness and convergence of the AO algorithm. Subsequently, we investigate the EE performance versus the distance between the BS and the IRS which is denoted as dr. As we can see in Fig. 4(a), EE first decreases and then increases as dr increases, which means when the IRS is closer to the BS or users, the value of EE is larger. The reason is that the channel gains of the IRS-aided links are determined by the distance-dependent path loss model, which can be written as $P_{IL} = C_0 dr^{-2} C_0 (6 - dr)^{-2.5}$, as shown in Fig. 4(b). Obviously, Fig.4(a) and Fig. 4(b) have the same trend since higher total achievable rates and larger total harvested energy can be obtained by larger channel gain. These results indicate that the system EE can be enhanced by the appropriate IRS placement.

Next, the effect of the number of transmit antennas on the EE is then investigated in different cases containing: 1) Conventional MISO SWIPT system without IRS [42], 2) Proposed system with random IRS phase shift, 3) Proposed

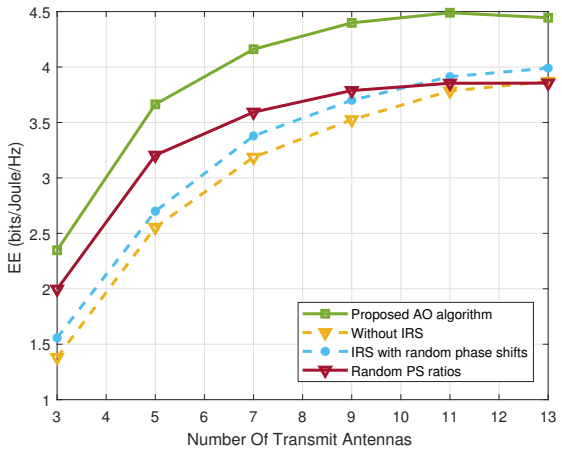

Fig. 5. EE versus the numbers of transmit antennas.

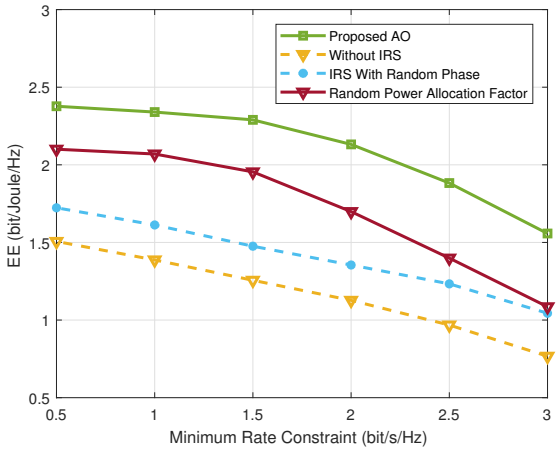

Fig. 6. EE versus minimum rate constraint per user.

system with random PS ratios for comparison. It can be observed in Fig. 5, EE increases rapidly when the number of antennas is relatively small. This is because as M increases, higher spatial diversity gain and beamforming gain can be obtained, thus yielding higher transmission rates and harvested energy. On the other hand, activating more transmit antennas will result in additional energy consumption, leading to some loss of EE. Therefore, the increase in EE becomes slower with a relatively large number of antennas, and a saturation will occur when the influence of the total achievable rate and the total power consumption on EE can offset each other. Meanwhile, when $M > 11$, EE achieved by the proposed algorithm even decreases slightly. This infers that in this case, the extra circuit power grows faster than the total achievable rate. A similar performance trend is also reflected in [43], [44]. It is obvious that the proposed AO algorithm can achieve higher EE as compared to the other three schemes owing to its capability of utilizing the transmit power effectively. In other words, by optimizing the reflective beamforming and the PS ratios, the AO algorithm can make the signal transmission environment more favorable, thus outperforming the other three schemes. In particular, the EE of the proposed system with IRS is at least 15% larger than the one without IRS when $M = 13$, which indicates the benefit of deploying IRS for enhancing the EE performance.

In the next simulation, we gradually increase the minimum rate constraint to investigate its effect on EE. It can be seen in Fig. 6 that the EE achieved by all the schemes declines as R_{min} increases. This is due to the fact that when R_{min} increases, the system will assign more power to ID, thus reducing the total harvested energy. Furthermore, for a large value of R_{min}, extra transmit power needs to be transmitted by the BS to meet the minimum rate constraints, thus magnifying the interference, which results in an imbalance between the denominator (the total power consumption) and the numerator (the total achievable rate) of the EE metric.

We next analyze the impact of the circuit power P_c to EE by setting P_c from 1W to 3.5W. As we can see in Fig. 7, EE declines as P_c increases for the AO algorithm and the other

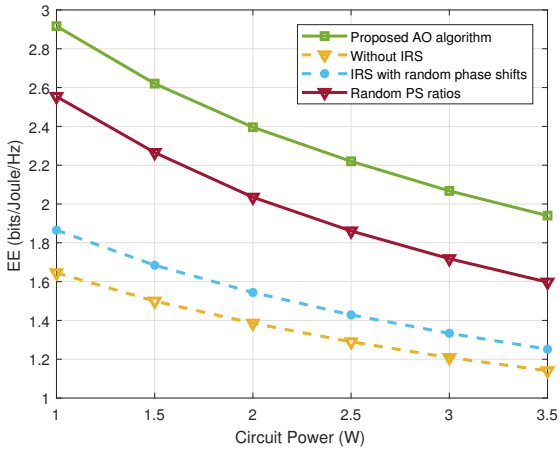

Fig. 7. EE versus circuit power of the proposed system.

three schemes. The reason is that the increase in the circuit power will directly increase the total power consumption, but has no effect on the total transmission rate of the system, thus resulting in a decrease in EE. Similar to the previous results, we can observe that the proposed AO algorithm performs better than the other three schemes.

We further investigate the effect of the number of reflecting units at the IRS on the EE performance versus circuit power. As shown in Fig. 8 that for N ranging from 4 to 32, EE gradually decreases as P_c increases. In addition, comparing the four curves in Fig. 8, the value of EE increases with the number of reflecting units. This is due to the fact that the design of the reflective beamforming vectors for EE maximization can become more flexible with a larger number of N. That is to say, the users can obtain higher passive beamforming gain, thus leading to a higher total transmission rate. Otherwise, since the IRS reflecting units are passive, even if N increases, the power consumed by the additional reflecting units is relatively low (0.01W per reflecting unit) compared to the total power consumption of the system. Therefore, with a higher total transmission rate and a lightly increased total

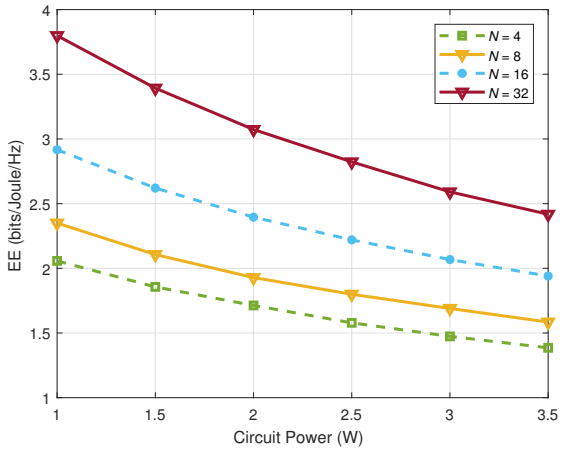

Fig. 8. EE versus circuit power of the proposed system.

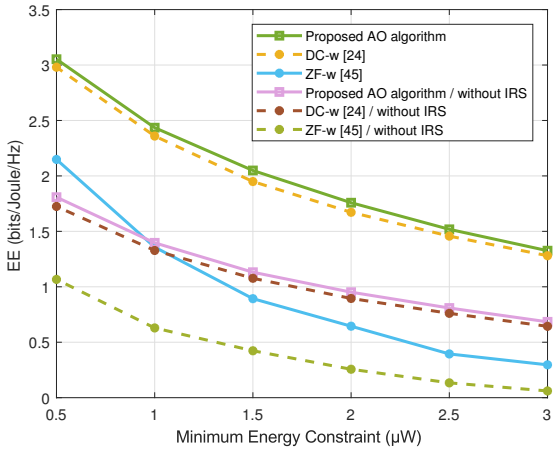

Fig. 10. EE versus minimum energy constraint per user.

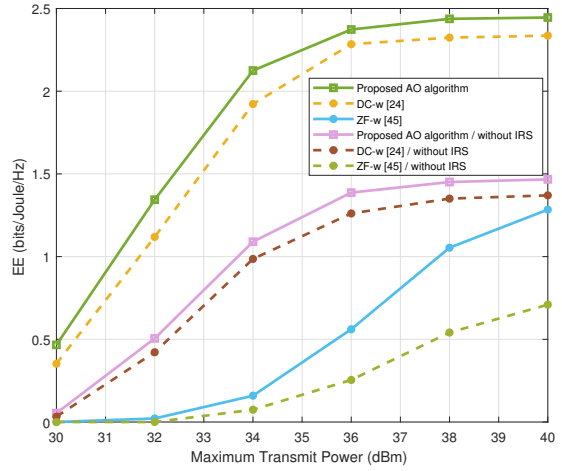

Fig. 9. EE versus maximum transmit power.

power consumption, the EE performance can be improved significantly.

Next, we propose two benchmark schemes marked as "DC-w" and "ZF-w", in which we apply the DC programming [24] and zero-forcing (ZF) [45] to optimize the BS transmit beamforming vectors, respectively. In addition, we also analyze the case where the SWIPT system without IRS deployed. As we can see in Fig. 9, for our proposed AO algorithm, EE first increases and then reaches an asymptotic value as P_T increases. The reason is that with a large value of P_T, the excessive power transmitted by the BS has no effect on EE, which means the balance between the total power consumption and the total achievable rate of the system is obtained. In addition, it can be seen in Fig. 10 that the EE achieved by all the schemes is monotonically decreasing in E_{min}. This is because, for a large value of E_{min}, the PS ratios need to decrease to meet the harvested energy demand. In other words, more power is needed to be allocated to EH, and thus leads to a decline in the achievable transmission rate. In addition, it can be seen from Fig. 9 and Fig. 10 that the proposed AO algorithm can achieve higher EE as compared to the other two benchmark schemes, which reflects the superiority of our algorithm. Furthermore, for all the schemes, the EE performance of the proposed system with IRS outperforms the one without IRS, which demonstrates the advantage of deploying IRS.

V. Conclusion

In this paper, we maximize the EE of a multiuser IRS-aided MISO system with SWIPT, while satisfying the BS transmit power constraints, the IRS reflection constraint, and the QoS constraints of each user. As the optimization variables, i.e., the transmit beamforming vectors, the reflective beamforming vector, and the PS ratios are intricately coupled, the original problem is extremely complex and non-convex. To effectively tackle the problem, we propose an AO algorithm by decoupling the original problem into three subproblems. Therefore, we apply the Dinkelbach method as well as SDR and SCA techniques to solve the subproblems. Finally, compared with the benchmarks, the effectiveness and the convergence of our proposed AO algorithm and the benefit of deploying IRS can be validated by numerical results. In addition, our work can be extended to a more realistic case by taking into account the imperfect CSI and the IRS hardware designs such as holographic multiple input multiple output surface (HMIMOS), which will be considered in our future work.

Appendix A
Proof of Theorem 1

Since problem (P2.2) is strictly convex in $\{\boldsymbol{W}_k\}$, the Slater's condition holds. Hence, the duality gap is zero. We can write the Lagrangian function corresponding to problem (P2.2) as

$$\begin{aligned}\mathscr{L} =& -\sum_{k=1}^{K}(p_k-q_k)\log_2(e)+q(\zeta\sum_{k=1}^{K}\mathrm{Tr}(\boldsymbol{W}_k)+P_C+MP_M\\ &+NP_n(b)-\sum_{k=1}^{K}\eta(1-\rho_k)\sum_{i=1}^{K}\mathrm{Tr}(\boldsymbol{A}_k\boldsymbol{W}_i))\\ &+\sum_{k=1}^{K}v_k(e^{p_k}-(\rho_k\sum_{i=1}^{K}\mathrm{Tr}(\boldsymbol{A}_k\boldsymbol{W}_i)+\sigma_k^2))\\ &+\sum_{k=1}^{K}u_k(\rho_k\sum_{i=1,i\neq k}^{K}\mathrm{Tr}(\boldsymbol{A}_k\boldsymbol{W}_i)+\sigma_k^2-(e^{\bar{q}_k}+e^{\bar{q}_k}(q_k-\bar{q}_k)))\\ &+\sum_{k=1}^{K}\lambda_k(R_{\min}-(p_k-q_k)\log_2(e))\\ &+\sum_{k=1}^{K}\tau_k(E_{\min}-\eta(1-\rho_k)\sum_{i=1}^{K}\mathrm{Tr}(\boldsymbol{A}_k\boldsymbol{W}_i))\\ &+\upsilon(\sum_{k=1}^{K}\mathrm{Tr}(\boldsymbol{W}_k)-P_T)-\sum_{k=1}^{K}\mathrm{Tr}(\boldsymbol{Y}_k\boldsymbol{W}_k),\end{aligned} \tag{69}$$

where $\{v_k\},\{u_k\},\{\lambda_k\},\{\tau_k\},\upsilon$ represent the Lagrangian multipliers, and $\{\boldsymbol{Y}_k\}\in\mathbb{C}^{\mathrm{M}\times\mathrm{M}}$ represents the Lagrangian multiplier matrix.

Therefore, we can express the dual problem of (P2.2) as

$$\max_{\{v_k^*\},\{u_k^*\},\{\lambda_k^*\},\{\tau_k^*\},\upsilon^*>0,\{\boldsymbol{Y}_k^*\}}\ \min_{\{\boldsymbol{W}_k\},\{p_k\},\{q_k\}}\mathscr{L}. \tag{70}$$

Let $\{v_k^*\},\{u_k^*\},\{\lambda_k^*\},\{\tau_k^*\},\upsilon*$ and $\{\boldsymbol{Y}_k^*\}$ denote the optimal Lagrangian multiplers of (70). Therefore, the Karush-Kuhn-Tucker (KKT) condition related to $\{\boldsymbol{W}_k^*\}$ is

$$K1:\{\boldsymbol{Y}_k^*\}\succeq\boldsymbol{0},\{v_k^*\},\{u_k^*\},\{\lambda_k^*\},\{\tau_k^*\},\upsilon^*>0, \tag{71}$$

$$K2:\boldsymbol{W}_k^*\boldsymbol{Y}_k^*=\boldsymbol{0},\forall k\in\mathcal{K}, \tag{72}$$

$$K3:\nabla_{\boldsymbol{W}_k^*}\mathscr{L}=0,\forall k\in\mathcal{K}, \tag{73}$$

where $\nabla_{\boldsymbol{W}_k^*}\mathscr{L}$ is the gradient vector of Eq. (69) with respect to $\{\boldsymbol{W}_k^*\}$, which can be written as

$$\begin{aligned}\nabla_{\boldsymbol{W}_k^*}\mathscr{L}=&\,q\zeta\boldsymbol{I}_M-q\sum_{i=1}^{K}\eta(1-\rho_i)\boldsymbol{A}_i-\sum_{i=1}^{K}v_i^*\rho_i\boldsymbol{A}_i+\\ &\sum_{i=1,i\neq k}^{K}u_i^*\rho_i\boldsymbol{A}_i-\sum_{i=1}^{K}\tau_i^*\eta(1-\rho_i)\boldsymbol{A}_i+\upsilon^*\boldsymbol{I}_M-\boldsymbol{Y}_k^*=0.\end{aligned} \tag{74}$$

For brevity, we can express $K3$ as

$$\boldsymbol{Y}_k^*=(q\zeta+\upsilon^*)\boldsymbol{I}_M-\mathrm{Z}_k \tag{75}$$

where Z_k can be given by $\sum_{i=1}^{K}v_i^*\rho_i\boldsymbol{A}_i-\sum_{i=1,i\neq k}^{K}u_i^*\rho_i\boldsymbol{A}_i+\sum_{i=1}^{K}\tau_i^*\eta(1-\rho_i)\boldsymbol{A}_i+q\sum_{i=1}^{K}\eta(1-\rho_i)\boldsymbol{A}_i$,

Next, we will prove that the optimal solution $\boldsymbol{W}_k^*$ of the problem (P2.2) satisfies $\mathrm{rank}(\boldsymbol{W}_k^*)=1,\forall k\in\mathcal{K}$ by analyzing the structure of $\boldsymbol{Y}_k^*$. Let $\xi_{\max}$ represent the maximum eigenvalue of Z_k. Due to the randomness of the channel, it is almost impossible for multiple eigenvalues to have the same maximum value. In light of the rank property of the matrices and $K2$, we obtain

$$\mathrm{rank}\,(\boldsymbol{Y}_k^*)+\mathrm{rank}\,(\boldsymbol{W}_k^*)\leq M. \tag{76}$$

If $\xi_{\max}>q\zeta+\upsilon^*$, an eigenvalue of $\boldsymbol{Y}_k^*$ will be negative, i.e., $\boldsymbol{Y}_k^*$ cannot be positive semidefinite, which is contradictory to $K1$. If $\xi_{\max}<q\zeta+\upsilon^*$, all the eigenvalues of $\boldsymbol{Y}_k^*$ will be positive, i.e.,$\boldsymbol{Y}_k^*$ must be full rank and positive definite. Furthermore, $K2$ informs us that $\boldsymbol{W}_k^*$ can only be $\boldsymbol{0}$, which contradicts the reality. Hence, $\xi_{\max}=q\zeta+\upsilon^*$ must hold, then $\mathrm{rank}\,(\boldsymbol{Y}_k^*)=M-1$. Therefore, $\mathrm{rank}\,(\boldsymbol{W}_k^*)=1$ must be satisfied.

Appendix B
Proof of Theorem 2

Above all, we introduce two sets of new variables as

$$S_k=\sum_{i=1}^{K}\left|(\boldsymbol{v}^H\boldsymbol{\Phi}_k+\boldsymbol{h}_k^H)\boldsymbol{w}_i\right|^2,\forall k\in\mathcal{K}, \tag{77}$$

$$T_k=\sum_{i=1,i\neq k}^{K}\left|\left(\boldsymbol{v}^H\boldsymbol{\Phi}_k+\boldsymbol{h}_k^H\right)\boldsymbol{w}_i\right|^2,\forall k\in\mathcal{K}, \tag{78}$$

$$\begin{aligned}C=q(&\zeta\sum_{k=1}^{K}\|\boldsymbol{w}_k\|^2+P_C+MP_M+NP_n(b)\\ &-\eta\sum_{k=1}^{K}\sum_{i=1}^{K}\left|\left(\boldsymbol{v}^H\boldsymbol{\Phi}_k+\boldsymbol{h}_k^H\right)\boldsymbol{w}_i\right|^2).\end{aligned} \tag{79}$$

Thus, (53) can be reformulated as

$$R(\boldsymbol{\rho})=\sum_{k=1}^{K}\log_2\left(\frac{\rho_kS_k+\sigma_k^2}{\rho_kT_k+\sigma_k^2}\right)-q\sum_{k=1}^{K}\eta\rho_kS_k-C. \tag{80}$$

Then we can write the first-order derivative of $R(\boldsymbol{\rho})$ as

$$\begin{aligned}\frac{\partial R(\boldsymbol{\rho})}{\partial\rho_m}=&\frac{1}{\ln 2}\frac{\rho_mT_m+\sigma_m^2}{\rho_mS_m+\sigma_m^2}\\ &\times\frac{S_m(\rho_mT_m+\sigma_m^2)-T_m(\rho_mS_m+\sigma_m^2)}{(\rho_mT_m+\sigma_m^2)^2}-q\eta S_m\\ =&\frac{1}{\ln 2}\frac{(S_m-T_m)\sigma_m^2}{(\rho_mS_m+\sigma_m^2)(\rho_mT_m+\sigma_m^2)}-q\eta S_m.\end{aligned} \tag{81}$$

Furthermore, the second-order derivative of $R(\boldsymbol{\rho})$ can be written as

$$\begin{aligned}&\frac{\partial^2R(\boldsymbol{\rho})}{\partial\rho_m\partial\rho_n}\\ &=\begin{cases}-\frac{1}{\ln 2}\frac{(S_m-T_m)\sigma_m^2(2S_mT_m\rho_m+(S_m+T_m)\sigma_m^2)}{(\rho_mS_m+\sigma_m^2)^2(\rho_mT_m+\sigma_m^2)^2} & <0,m=n.\\ 0,m\neq n\end{cases}\end{aligned} \tag{82}$$

Therefore, we can express the Hessian matrix of $R(\boldsymbol{\rho})$ as

$$\frac{\partial R(\boldsymbol{\rho})}{\partial\boldsymbol{\rho}^2}=\begin{bmatrix}\frac{\partial R(\boldsymbol{\rho})}{\partial\rho_1^2} & 0 & \cdots & 0\\ 0 & \frac{\partial R(\boldsymbol{\rho})}{\partial\rho_2^2} & \cdots & 0\\ \vdots & \vdots & \ddots & \vdots\\ 0 & 0 & \cdots & \frac{\partial R(\boldsymbol{\rho})}{\partial\rho_2^2}\end{bmatrix}. \tag{83}$$

It is obvious that $\frac{\partial R(\boldsymbol{\rho})}{\partial \rho_k^2} < 0$, which means $\frac{\partial R(\boldsymbol{\rho})}{\partial \boldsymbol{\rho}^2}$ is a negative semi-definite matrix. Consequently, the objective function (53) is strictly concave in $\rho_k, \forall k \in \mathcal{K}$.

REFERENCES

[1] Q. Wu, G. Y. Li, W. Chen, D. W. K. Ng, and R. Schober, "An overview of sustainable green 5G networks," *IEEE Wireless Communications*, vol. 24, no. 4, pp. 72–80, 2017.

[2] W. Saad, M. Bennis, and M. Chen, "A vision of 6G wireless systems: Applications, trends, technologies, and open research problems," *IEEE Network*, vol. 34, no. 3, pp. 134–142, 2020.

[3] Q. Wu and R. Zhang, "Towards smart and reconfigurable environment: Intelligent reflecting surface aided wireless network," *IEEE Communications Magazine*, vol. 58, no. 1, pp. 106–112, 2020.

[4] Q. Wu, S. Zhang, B. Zheng, C. You, and R. Zhang, "Intelligent reflecting surface-aided wireless communications: A tutorial," *IEEE Transactions on Communications*, vol. 69, no. 5, pp. 3313–3351, 2021.

[5] Q. Wu and R. Zhang, "Intelligent reflecting surface enhanced wireless network via joint active and passive beamforming," *IEEE Transactions on Wireless Communications*, vol. 18, no. 11, pp. 5394–5409, 2019.

[6] S. Zhang and R. Zhang, "Capacity characterization for intelligent reflecting surface aided MIMO communication," *IEEE Journal on Selected Areas in Communications*, vol. 38, no. 8, pp. 1823–1838, 2020.

[7] C. Pan, H. Ren, K. Wang, W. Xu, M. Elkashlan, A. Nallanathan, and L. Hanzo, "Multicell MIMO communications relying on intelligent reflecting surfaces," *IEEE Transactions on Wireless Communications*, vol. 19, no. 8, pp. 5218–5233, 2020.

[8] Y. Lee, J.-H. Lee, and Y.-C. Ko, "Beamforming optimization for IRS-assisted mmWave V2I communication systems via reinforcement learning," *IEEE Access*, vol. 10, pp. 60521–60533, 2022.

[9] Y. Xiu, Y. Zhao, Y. Liu, J. Zhao, O. Yagan, and N. Wei, "IRS-assisted millimeter wave communications: Joint power allocation and beamforming design," in *2021 IEEE Wireless Communications and Networking Conference Workshops (WCNCW)*, pp. 1–6, 2021.

[10] Y. Guo, G. Liu, J. Ren, Y. Liu, L. Yao, Y. Cao, J. Chen, and Y. Zhou, "Physical layer security of IRS-assisted multi-layer heterogeneous networks in smart grid," in *2022 International Conference on Computing, Communication, Perception and Quantum Technology (CCPQT)*, pp. 128–134, 2022.

[11] Y. Xu, H. Xie, Q. Wu, C. Huang, and C. Yuen, "Robust max-min energy efficiency for RIS-aided hetnets with distortion noises," *IEEE Transactions on Communications*, vol. 70, no. 2, pp. 1457–1471, 2022.

[12] C. Huang, Z. Yang, G. C. Alexandropoulos, K. Xiong, L. Wei, C. Yuen, Z. Zhang, and M. Debbah, "Multi-hop RIS-empowered terahertz communications: A DRL-based hybrid beamforming design," *IEEE Journal on Selected Areas in Communications*, vol. 39, no. 6, pp. 1663–1677, 2021.

[13] S. Dash, C. Psomas, I. Krikidis, I. F. Akyildiz, and A. Pitsillides, "Active control of THz waves in wireless environments using graphene-based RIS," *IEEE Transactions on Antennas and Propagation*, vol. 70, no. 10, pp. 8785–8797, 2022.

[14] Z. Wei, Y. Cai, Z. Sun, D. W. K. Ng, J. Yuan, M. Zhou, and L. Sun, "Sum-rate maximization for IRS-assisted UAV OFDMA communication systems," *IEEE Transactions on Wireless Communications*, vol. 20, no. 4, pp. 2530–2550, 2021.

[15] A. Mahmoud, S. Muhaidat, P. C. Sofotasios, I. Abualhaol, O. A. Dobre, and H. Yanikomeroglu, "Intelligent reflecting surfaces assisted UAV communications for IoT networks: Performance analysis," *IEEE Transactions on Green Communications and Networking*, vol. 5, no. 3, pp. 1029–1040, 2021.

[16] H. Lee, K.-J. Lee, H. Kim, and I. Lee, "Joint transceiver optimization for MISO SWIPT systems with time switching," *IEEE Transactions on Wireless Communications*, vol. 17, no. 5, pp. 3298–3312, 2018.

[17] J. Tang, J. Luo, M. Liu, D. K. C. So, E. Alsusa, G. Chen, K.-K. Wong, and J. A. Chambers, "Energy efficiency optimization for NOMA with SWIPT," *IEEE Journal of Selected Topics in Signal Processing*, vol. 13, no. 3, pp. 452–466, 2019.

[18] Z. Zong, H. Feng, F. R. Yu, N. Zhao, T. Yang, and B. Hu, "Optimal transceiver design for SWIPT in k-user MIMO interference channels," *IEEE Transactions on Wireless Communications*, vol. 15, no. 1, pp. 430–445, 2016.

[19] Y. Huang, M. Liu, and Y. Liu, "Energy-efficient SWIPT in IoT distributed antenna systems," *IEEE Internet of Things Journal*, vol. 5, no. 4, pp. 2646–2656, 2018.

[20] D. Xu and H. Zhu, "Outage minimized resource allocation for multiuser OFDM systems with SWIPT," *IEEE Access*, vol. 7, pp. 79714–79725, 2019.

[21] K. Agrawal, S. Prakriya, and M. F. Flanagan, "Optimization of SWIPT with battery-assisted energy harvesting full-duplex relays," *IEEE Transactions on Green Communications and Networking*, vol. 5, no. 1, pp. 243–260, 2021.

[22] Q. Wu and R. Zhang, "Weighted sum power maximization for intelligent reflecting surface aided SWIPT," *IEEE Wireless Communications Letters*, vol. 9, no. 5, pp. 586–590, 2020.

[23] S. Zargari, S. Farahmand, B. Abolhassani, and C. Tellambura, "Robust active and passive beamformer design for IRS-aided downlink MISO PS-SWIPT with a nonlinear energy harvesting model," *IEEE Transactions on Green Communications and Networking*, vol. 5, no. 4, pp. 2027–2041, 2021.

[24] S. Zargari, A. Khalili, and R. Zhang, "Energy efficiency maximization via joint active and passive beamforming design for multiuser MISO IRS-aided SWIPT," *IEEE Wireless Communications Letters*, vol. 10, no. 3, pp. 557–561, 2021.

[25] Z. Li, W. Chen, Q. Wu, K. Wang, and J. Li, "Joint beamforming design and power splitting optimization in IRS-assisted SWIPT NOMA networks," *IEEE Transactions on Wireless Communications*, vol. 21, no. 3, pp. 2019–2033, 2022.

[26] Z. Yang and Y. Zhang, "Beamforming optimization for RIS-aided SWIPT in cell-free MIMO networks," *China Communications*, vol. 18, no. 9, pp. 175–191, 2021.

[27] J. Liu, K. Xiong, Y. Lu, D. W. K. Ng, Z. Zhong, and Z. Han, "Energy efficiency in secure IRS-aided SWIPT," *IEEE Wireless Communications Letters*, vol. 9, no. 11, pp. 1884–1888, 2020.

[28] V. Sharma, J. Yaswanth, S. K. Singh, S. Biswas, K. Singh, and F. Khan, "A pricing-based approach for energy-efficiency maximization in RIS-aided multi-user MIMO SWIPT-enabled wireless networks," *IEEE Access*, vol. 10, pp. 29132–29148, 2022.

[29] X. Zhou, R. Zhang, and C. K. Ho, "Wireless information and power transfer: Architecture design and rate-energy tradeoff," *IEEE Transactions on Communications*, vol. 61, no. 11, pp. 4754–4767, 2013.

[30] M. Grant, S. Boyd, and Y. Ye, "CVX: Matlab software for disciplined convex programming," 2008.

[31] M. Jian, G. C. Alexandropoulos, E. Basar, C. Huang, R. Liu, Y. Liu, and C. Yuen, "Reconfigurable intelligent surfaces for wireless communications: Overview of hardware designs, channel models, and estimation techniques," *Intelligent and Converged Networks*, vol. 3, no. 1, pp. 1–32, 2022.

[32] L. Wei, C. Huang, G. C. Alexandropoulos, C. Yuen, Z. Zhang, and M. Debbah, "Channel estimation for RIS-empowered multi-user MISO wireless communications," *IEEE Transactions on Communications*, vol. 69, no. 6, pp. 4144–4157, 2021.

[33] X. Lu, P. Wang, D. Niyato, D. I. Kim, and Z. Han, "Wireless networks with RF energy harvesting: A contemporary survey," *IEEE Communications Surveys & Tutorials*, vol. 17, no. 2, pp. 757–789, 2015.

[34] X. Di, K. Xiong, P. Fan, and H.-C. Yang, "Simultaneous wireless information and power transfer in cooperative relay networks with rateless codes," *IEEE Transactions on Vehicular Technology*, vol. 66, no. 4, pp. 2981–2996, 2017.

[35] C. Huang, A. Zappone, G. C. Alexandropoulos, M. Debbah, and C. Yuen, "Reconfigurable intelligent surfaces for energy efficiency in wireless communication," *IEEE Transactions on Wireless Communications*, vol. 18, no. 8, pp. 4157–4170, 2019.

[36] W. Dinkelbach, "On nonlinear fractional programming," *Management science*, vol. 13, no. 7, pp. 492–498, 1967.

[37] Z.-q. Luo, W.-k. Ma, A. M.-c. So, Y. Ye, and S. Zhang, "Semidefinite relaxation of quadratic optimization problems," *IEEE Signal Processing Magazine*, vol. 27, no. 3, pp. 20–34, 2010.

[38] B. Lyu, P. Ramezani, D. T. Hoang, S. Gong, Z. Yang, and A. Jamalipour, "Optimized energy and information relaying in self-sustainable IRS-empowered WPCN," *IEEE Transactions on Communications*, vol. 69, no. 1, pp. 619–633, 2021.

[39] S. Zargari, A. Khalili, Q. Wu, M. Robat Mili, and D. W. K. Ng, "Max-min fair energy-efficient beamforming design for intelligent reflecting surface-aided SWIPT systems with non-linear energy harvesting model," *IEEE Transactions on Vehicular Technology*, vol. 70, no. 6, pp. 5848–5864, 2021.

[40] H. Xie, J. Xu, and Y.-F. Liu, "Max-min fairness in IRS-aided multi-cell MISO systems with joint transmit and reflective beamforming," *IEEE Transactions on Wireless Communications*, vol. 20, no. 2, pp. 1379–1393, 2021.

[41] H. Guo, Y.-C. Liang, J. Chen, and E. G. Larsson, "Weighted sum-rate maximization for reconfigurable intelligent surface aided wireless networks," *IEEE Transactions on Wireless Communications*, vol. 19, no. 5, pp. 3064–3076, 2020.

[42] J. Tang, D. K. C. So, N. Zhao, A. Shojaeifard, and K.-K. Wong, "Energy efficiency optimization with SWIPT in MIMO broadcast channels for internet of things," *IEEE Internet of Things Journal*, vol. 5, no. 4, pp. 2605–2619, 2018.

[43] V. Khodamoradi, A. Sali, O. Messadi, A. A. Salah, M. M. Al-Wani, B. M. Ali, and R. S. A. R. Abdullah, "Optimal energy efficiency based power adaptation for downlink multi-cell massive MIMO systems," *IEEE Access*, vol. 8, pp. 203237–203251, 2020.

[44] J. Tang, A. Shojaeifard, D. K. C. So, K.-K. Wong, and N. Zhao, "Energy efficiency optimization for CoMP-SWIPT heterogeneous networks," *IEEE Transactions on Communications*, vol. 66, no. 12, pp. 6368–6383, 2018.

[45] Q. Shi, C. Peng, W. Xu, M. Hong, and Y. Cai, "Energy efficiency optimization for MISO SWIPT systems with zero-forcing beamforming," *IEEE Transactions on Signal Processing*, vol. 64, no. 4, pp. 842–854, 2016.